Neural-Mechanical Feedback Control Scheme Generates Physiological Ankle Torque Fluctuation during Quiet Stance

Running Title: Neural-Mechanical Control Scheme of Quiet Stance

Authors:

Albert H. Vette[1,2], *Student Member, IEEE*, Kei Masani[1,2], Kimitaka Nakazawa[3], and Milos R. Popovic[1,2], *Senior Member, IEEE*.

Affiliations:

[1] Institute of Biomaterials and Biomedical Engineering, University of Toronto, 164 College Street, Toronto, Ontario, M5S 3G9, Canada

[2] Toronto Rehabilitation Institute, Lyndhurst Centre, 520 Sutherland Drive, Toronto, Ontario, M4G 3V9, Canada

[3] Department of Rehabilitation for Movement Functions, National Rehabilitation Center for Persons with Disabilities, 4-1 Namiki, Tokorozawa 359-8555, Japan

November 6, 2009

Corresponding Author:

Albert H. Vette, Dipl.-Ing.
Rehabilitation Engineering Laboratory, Lyndhurst Centre
Toronto Rehabilitation Institute
520 Sutherland Drive, Toronto, Ontario, M4G 3V9, Canada
Phone: +1-416-964-7145 / Fax: +1-416-425-9923
Email: a.vette@utoronto.ca
www.toronto-fes.ca

ABSTRACT

We have recently demonstrated in simulations and experiments that a proportional and derivative (PD) feedback controller can regulate the active ankle torque during quiet stance and stabilize the body despite a long sensory-motor time delay. The purpose of the present study was to: 1) model the active and passive ankle torque mechanisms and identify their contributions to the total ankle torque during standing; and 2) investigate whether a neural-mechanical control scheme that implements the PD controller as the neural controller can successfully generate the total ankle torque as observed in healthy individuals during quiet stance. Fourteen young subjects were asked to stand still on a force platform to acquire data for model optimization and validation. During two trials of 30 s each, the fluctuation of the body angle, the electromyogram of the right soleus muscle, and the ankle torque were recorded. Using these data, the parameters of: 1) the active and passive torque mechanisms (Model I); and 2) the PD controller within the neural-mechanical control scheme (Model II) were optimized to achieve potential matching between the measured and predicted ankle torque. The performance of the two models was finally validated with a new set of data. Our results indicate that not only the passive, but also the active ankle torque mechanism contributes significantly to the total ankle torque and, hence, to body stabilization during quiet stance. In addition, we conclude that the proposed neural-mechanical control scheme successfully mimics the physiological control strategy during quiet stance and that a PD controller is a legitimate model for the strategy that the central nervous system applies to regulate the active ankle torque in spite of a long sensory-motor time delay.

INDEX TERMS – Ankle torque, functional electrical stimulation, proportional and derivative (PD) feedback control, quiet standing, sensory-motor time delay.

I. INTRODUCTION

The lost ability of individuals with spinal cord injury (SCI) to stand can be regained by artificially stimulating the skeletal muscles in the lower limbs [1]. Recently, *arm-free* standing of individuals with SCI using functional electrical stimulation (FES) has drawn much attention in the field as it might allow individuals with SCI to stand and use both arms to perform activities of daily living (ADL) [2], [3]. However, current FES systems do not open up this possibility yet. Instead, they require that the person actively regulates balance using at least one arm, thus, limiting the use of the FES systems during ADL [4], [5].

The lack of knowledge of an effective closed-loop control strategy to regulate FES induced muscle contractions might also be due to an insufficient understanding of the control strategy that healthy individuals apply during quiet stance. Since the dynamics of quiet standing can be approximated by an inverted pendulum [6], the primary purpose of the control system during quiet stance is to provide the ankle torque needed to resist the gravity effect of the body and to ensure that its center of mass (COM) remains close to the equilibrium position. We do know that the ankle joint torque needed to stabilize the body can be evoked passively and actively. The *passive torque component* results from intrinsic mechanical properties of the joints, muscles, and ligaments (stiffness and damping), whereas the *active torque component* is generated via ankle muscle contractions that are regulated by the central nervous system (CNS). While passive torque alone cannot prevent the body from falling forward [7]-[9], it is still unclear how the CNS controls the ankle muscles to generate a timely active torque fluctuation despite a long *sensory-motor time delay* in the neural control mechanism. Note that the sensory-motor time delay, which should not only include the commonly considered transmission time delays [10]-[13], but also a delay due to the actual torque generation process [14], threatens the

stability of the system.

On the one hand, a *feed-forward* control mechanism has been hypothesized to successfully compensate for the sensory-motor time delay and regulate the active ankle torque during quiet standing [12], [13], [15]-[20]. On the other hand, also a linear *feedback* controller has been considered to represent the postural control mechanism during upright stance [21], [22]. In this context, our team showed that a feedback system regulated by a proportional and derivative (PD) controller can represent the neural control scheme that the CNS applies to generate the active torque and promote ankle joint stabilization despite the sensory-motor time delay [14], [23], [24]. In addition, we verified in experiments with a subject with a rare neurological disorder that the implemented PD controller can, in fact, improve balance during standing and facilitate quiet standing dynamics observed in healthy individuals [25].

To further validate our previous results and at the same time provide a more comprehensive model of the control system during quiet stance, the purpose of the present study was to: 1) model the active and passive ankle torque mechanisms and identify their contributions to the total ankle torque during standing; and 2) investigate whether a neural-mechanical control scheme that implements the PD controller as the neural controller can successfully generate the total ankle torque as observed in healthy individuals during quiet stance.

II. METHODS

A. *Physiological Control Concept of Quiet Standing*

Fig. 1 depicts a model of the control concept of quiet stance. The passive torque depends on the rotational stiffness and damping of the ankle joints, muscles, and ligaments (*mechanical controller*), whereas the active torque is regulated by the CNS via sensory information on the body kinematics (*neural controller*) and generated by the contractile elements of the ankle muscles. Using this definition, the passive torque includes the torque due to the stiffness of the ankle joints and due to the stiffness of the active muscles.

Note that the neural feedback loop is affected by the sensory-motor time delay and needs to be compensated for by the neural controller. The sensory-motor time delay consists of:

- a constant feedback time delay that represents the time loss due to neural transmission from the ankle somatosensory system to the brain (τ_F);

- a constant motor command time delay, which represents the time loss due to the sensory-motor information process in the CNS and the neural transmission from the CNS to the plantar flexors (τ_M); and

- an electromechanical delay between muscle activation and active torque generation that results from the *neuro-musculo-skeletal dynamics* of the ankle joint complex (τ_E). Note that τ_E is a varying quantity that depends on the frequency spectrum of the neural input and the dynamic properties of the muscles and joint [14], [26].

B. *Model Identification*

Since the identification of the neuro-musculo-skeletal (NMS) dynamics from muscle activation to active torque generation as well as the gains of the mechanical controller should not

be affected by the proposed neural controller, these two components have to be studied independent of the neural control strategy. As such, in *Section IIB1*, the active and passive torque mechanisms will be identified, whereas in *Section IIB2*, the obtained results will be used to evaluate the ability of the previously proposed PD controller to represent the neural controller in the neural-mechanical control scheme of quiet standing.

1) Active and Passive Torque Mechanisms (Model I)

The model of the NMS dynamics and of the mechanical controller is shown in Fig. 2. Using muscle activity and body angle data from quiet standing experiments with able-bodied subjects, the model was expected to generate the active ankle torque as well as the mechanically controlled passive ankle torque during quiet standing. For each subject, the predicted torque fluctuation was then compared with respective experimental ankle torque data and optimized by tuning the parameters of the NMS dynamics (T and G in Fig. 2) and the stiffness component of the mechanical controller (K in Fig. 2).

In order to identify the NMS dynamics, it has to be known that the plantar flexors are responsible for generating the active ankle torque as they show continuous activity during quiet standing; the dorsiflexors on the other hand are at most intermittently active [23]. Among the plantar flexors, the activity of the soleus muscle (SOL) during quiet stance is about five times as large as that of the gastrocnemius muscle with respect to their overall capacities [27]. Additionally, the cross-sectional area of SOL is twice as large as that of the gastrocnemius muscle (medial and lateral heads together) [28]. Hence, we assumed that SOL is the dominant contributor to the active ankle torque generation and used its electromyogram (EMG_{SOL}) as the input to the NMS dynamics model. Note that the underlying assumption was indeed verified in one of our recent studies [14].

As seen in the upper dashed box of Fig. 2, the dynamics from EMG_{SOL} to the active ankle torque were modeled via a second-order low-pass system that has been used to capture the isometric activation-force relationship in cats [29], [30] and humans [30]-[34]. Especially the soleus muscle has been studied extensively via the second-order low-pass system, and this for more than three decades [29], [30], [33], [34]. Since the muscle length change is very small during quiet standing, i.e., less than 0.5 % of the full potential length change (0.6 mm in [16] compared to 140 mm in [35]), this model can also be used for the quiet standing task. In fact, we recently used a critically damped second-order model for the standing posture and demonstrated that the model can successfully approximate the ankle torque generation process during standing [14].

From a physiological perspective, the second-order dynamics represent the chemical dynamics for the variation of calcium concentration in the muscle fiber and the mechanical dynamics for the sliding filament action [36], [37]. The transfer function $H(s)$ is written as:

$$H(s)=\frac{G}{T^2s^2+2Ts+1},$$
(1)

where G is the gain and T the twitch contraction time of the second-order system [26]. Note that the twitch contraction time T is equivalent to the inverse of the system's natural frequency ($T=1/\omega_n$). While T in (1) characterizes the NMS dynamics of SOL, G depends on the location of the electrodes and the impedance between the electrodes and the skin. Therefore, G has no deeper physiological meaning in the context of the present study. As indicated in Fig. 2, the output of the NMS dynamics model was doubled to consider the active torque contribution from both legs (based on the assumption of symmetry).

The mechanical controller with gains for the rotational stiffness (K) and damping (B)

generated the total passive ankle torque based on the body angle fluctuation during quiet standing (lower dashed box in Fig. 2). While the stiffness gain K had to be identified, the damping gain was set to B = 5 Nms/rad (based on Loram and Lakie [8]) as both the contribution and variability of K have been shown to outrange B by a factor of about 100 [8]. Note that one advantage associated with keeping B constant is that the performed optimizations are computationally more efficient and the torque matching results more significant due to the lower number of variables.

2) Neural-Mechanical Control Scheme (Model II)

The model of the neural-mechanical control scheme of quiet standing is shown in Fig. 3. Using body angle data from the standing experiments, the feedback model was expected to generate the neurally controlled active ankle torque as well as the mechanically controlled passive ankle torque during quiet standing. For each subject, the predicted torque fluctuation was then compared with respective experimental ankle torque data and optimized by tuning the control gains of the neural controller (K_p and K_d in Fig. 3).

The neural controller was modeled as a PD controller (upper left dashed box in Fig. 3), whereas the values for T and K were taken from *Section B1* to adequately characterize the NMS dynamics (upper right dashed box in Fig. 3) and the stiffness component of the mechanical controller (lower dashed box in Fig. 3), respectively. Based on values reported in the literature, the feedback time delay and the motor command time delay were set to $\tau_F = 40$ ms [38] and $\tau_M = 40$ ms [39], respectively.

C.   Experimental Data Acquisition and Processing

In order to acquire the body angle, EMG_{SOL}, and ankle torque data, we performed quiet

standing experiments with fourteen young subjects (age 31.9 ± 5.1 years; height 174.9 ± 8.8 cm; weight 69.0 ± 10.2 kg). None of the subjects had any known history of neurological disorders. Each subject gave written informed consent to the experimental procedure, which was approved by the local ethics committee in accordance with the declaration of Helsinki on the use of human subjects in experiments.

Each subject was asked to maintain a quiet stance posture standing barefoot with eyes closed. Note that the eyes-closed condition was chosen over the eyes-open condition as it is in better agreement with the single-link inverted pendulum model of quiet standing [40]. To acquire sufficient data for model identification, two trials of 30 seconds were executed. During each trial, the subject was standing on a force platform (9281B, Kistler, Switzerland) that measured the fluctuation of the total ankle torque. Additionally, a laser displacement sensor (LK2500, Keyence, Japan) was placed behind the subject recording the anterior-posterior body sway fluctuation at the midpoint between the right ankle and knee joints. The activity of the right SOL (EMG$_{SOL}$) was amplified by a factor of 10,000 and band-pass filtered between 20 and 450 Hz (Bangnoli 8 EMG System, Delsys, USA).

All time series were logged at a sampling frequency of 1 kHz, an analog-to-digital (AD) resolution of 16 bit, and signal-specific, i.e., optimal voltage ranges (ML880 PowerLab 16/30, ADInstruments, USA). For optimal noise rejection, the AD converter was preceded by an analog anti-aliasing (low-pass) filter of fixed cut-off frequency (49 kHz) and followed by a digital finite-impulse-response filter with a cut-off frequency set to the Nyquist value (500 Hz). While the torque and body sway fluctuation were then low-pass filtered using a fourth-order, zero phase-lag Butterworth filter with a cut-off frequency of 2 Hz [26], EMG$_{SOL}$ was only rectified. Note that the rectified, unfiltered EMG$_{SOL}$ was used in the model of the active torque mechanism since

the NMS dynamics represent a transducer that convert neural input (surface-rectified EMG) to torque output [33]. Finally, the body sway recordings were converted into body angle data using the height of the laser above the ankle joint and the force plate measurements.

D.   Optimization and Validation Procedure

The data from the first of the two standing trials of each subject were used for the identification of the NMS dynamics and the stiffness gain of the mechanical controller (Fig. 2). In order to investigate whether a good matching between the measured and predicted ankle torque was possible, the parameters T, G, and K (gray boxes in Fig. 2) were optimized by means of the *DIRECT optimization technique* [41] (Matlab ver. 7.5 and Simulink ver. 7.0, Mathworks Inc., USA). This technique requires no knowledge of the objective function gradient; instead, the algorithm samples points in the domain and uses the obtained information to decide where to search next. T, G, and K were tuned within ranges of 0-1000 ms, 0-500 Nm/V, and 0-150 % of the subject's load stiffness, respectively. Note that the load stiffness of each subject, T_{LOAD}, is defined as:

$$T_{LOAD} = m_{body} \cdot g \cdot h_{COM} \ ,$$

(2)

where m_{body} is the mass of the body without the feet, g the acceleration due to gravity, and h_{COM} the height of the body's COM above the ankle joint [26]. The optimization procedure was terminated once the ankle torque error remained constant for 100 consecutive iterations, suggesting the detection of the error's global minimum. Following the optimization, the final values for T, G, and K were validated with a new set of experimental data from the second standing trial of each subject. For the optimizations and the evaluation of the optimized and

validated data, the goodness of fit between the measured and predicted ankle torque, *%Fit* [14],

was determined by calculating the average of the percentage errors for all samples using:

$$\% Fit = 100\,(1 - \frac{1}{N}\sum_{i=1}^{N}\left|\frac{y_i - Y_i}{y_i}\right|)\,,\qquad\qquad(3)$$

where N is the number of samples (30,000), y the measured and Y the predicted ankle torque.

Each subject's final values for T and K were then implemented in the model of the

neural-mechanical control scheme of quiet stance (Fig. 3). It was used to optimize the gains Kp

and Kd of the neural controller (gray boxes in Fig. 3) and validate the final values for all

parameters (T, K, Kp, and Kd) with a new set of data. The optimization procedure tuned the

gains Kp and Kd within the range of 0-150 % of the subject's load stiffness (T_{LOAD}) and was

again terminated once the ankle torque error remained constant for 100 consecutive iterations.

The experimental data from the first and second standing trials of each subject were used for the

optimization and validation, respectively. Finally, the goodness of fit between the measured and

predicted ankle torque was evaluated for both the optimized and validated data via (3).

E. *Methodological Verification*

1) *Parameter Robustness*

To determine the robustness of the parameter identification for all subjects and both

models, we studied the effect of 1) two different experimental data sets (body angle, EMG_{SOL},

and ankle torque); 2) three different cut-off frequencies of the experimental low-pass filter (2, 10,

and '∞' Hz, i.e., no filtering at all); and 3) three physiologically feasible values for the damping

gain B (0, 5, and 10 Nms/rad [8]). Potential differences in estimates within (main effects) and

between (interactions) the factors 'data set', 'cut-off frequency', and 'damping gain B' were

captured using a three-way ANOVA with repeated measures ($\alpha = 0.1$). Moreover, to evaluate

parameter differences between subjects, we compared the intra- and inter-subject variance of the parameter estimates using the 18 robustness optimizations described above (2*3*3).

2) Model Structure

In order to confirm the validity of the model structure, we evaluated whether the identified parameters (T, K, Kp, and Kd) along with the pre-set parameters (B = 5 Nms/rad, τ_F, and τ_M) would result in a stable system for all subjects. For this purpose, we implemented each subject's parameters in a previously proposed *closed-loop* feedback model of quiet stance regulating the subject's inverted pendulum model (*Fig. 2 in [14]*) and carried out Nyquist stability analysis using the *open-loop* model.

In addition to the stability analysis, we performed simulations with the closed-loop feedback model and external perturbations to show that our methodology is capable of reliably estimating the parameters of the model structure. Note that the applied (noise) perturbations were modeled as a low-pass filtered, uniform random number with zero mean and unity variance (*see Section 2.3.1. and Fig. 1 in [24] for further details*). Same as in our previous study [24], the perturbations were introduced as a continuous disturbance torque at the ankle joints, representing the summation of all internal noise. In a first step of this verification component, time series were generated for each subject (SOL motor command, body angle, and ankle torque) by means of the perturbed closed-loop feedback model and each subject's identified parameters T, K, Kp, and Kd. In a second step, the time series were used in the two optimization models described in *Section IIB* to re-estimate the parameters of the closed-loop feedback model (identical optimization procedure and settings as in *Section IID*).

III. RESULTS

A.   *Active and Passive Torque Mechanisms*

In Fig. 4, the experimental time series and the ankle torque predicted via the active and passive torque mechanisms (Fig. 2) are shown for one subject (validation). Figs. 4a and 4b depict the experimental body angle and EMG_{SOL} data, respectively. In Fig. 4c, the bold gray line represents the fluctuation of the experimental and the thin black line the fluctuation of the predicted ankle torque. It can be seen that the predicted ankle torque fitted the measured ankle torque very well. Fig. 4c also shows the predicted passive and active torque components using dashed and dotted lines, respectively.

The optimization and validation results for the active and passive torque mechanisms (Fig. 2) are summarized in the first part of Table I (Model I). The twitch contraction time T had an average value of 167 ms, implying a natural frequency of the second-order NMS dynamics model of approximately 6 rad/s. The mechanical stiffness gain K had an average value of 521 Nm/rad, which accounted for 83 % of the subjects' load stiffness (*%T_{LOAD}*). Finally, using the identified values for T, G, and K, the goodness of fit evaluation revealed a high level of matching between the measured and predicted ankle torque. For the optimization, the goodness of fit had an average value of 98.4 %, a minimum of 97.3 %, and a maximum of 99.2 %. For the validation, it had an average value of 96.7 %, a minimum of 87.9 %, and a maximum of 98.6 %. A paired t-test revealed that there was no difference in *%Fit* between the optimized and validated data (P = 0.056).

B.   *Neural-Mechanical Control Scheme*

In Fig. 5, examples of the total ankle torque fluctuation from the experiments and the simulations of the neural-mechanical control scheme (Fig. 3) are shown. Fig. 5a depicts the

fluctuations from the optimization trial and Fig. 5b the fluctuations from the validation trial. In each plot, the bold gray line marks the experimental ankle torque and the thin black line the predicted ankle torque using the mechanical and neural controllers. A visual inspection suggests that the predicted ankle torque closely matched the ankle torque measured during quiet stance. Note that both plots in Fig. 5 also show the predicted passive and active torque components using dashed and dotted lines, respectively.

The optimization and validation results for the model of the neural-mechanical control scheme (Fig. 3) are summarized in the second part of Table I (Model II). The neural controller's proportional gain Kp and derivative gain Kd had average values of 126 Nm/rad and 158 Nms/rad, respectively. Using the identified values for T, K, Kp, and Kd, the goodness of fit evaluation revealed a high level of matching between the measured and predicted ankle torque. For the optimization, the goodness of fit had an average value of 98.3 %, a minimum of 97.5 %, and a maximum of 98.9 %. For the validation, it had an average value of 96.6 %, a minimum of 85.3 %, and a maximum of 98.7 %. A paired t-test revealed that there was no difference in *%Fit* between the optimized and validated data (P = 0.112).

C. *Methodological Verification*

The three-way ANOVA performed with the parameter estimates obtained in the 18 robustness optimizations failed to reveal significant differences within and between factors (P>0.9) – and this for all five parameters T, G, K, Kp, and Kd. As such, there is no evidence that the fitting results were affected by the choice of data set, cut-off frequency, and damping gain B. Taking also into account that the intra-subject variation of the parameter estimates was much smaller than the inter-subject variation (SD ratios in last column of Table I), we conclude that the inter-subject variability reflects, in fact, differences among subjects and not simply a lack of

precision in the estimations.

Fig. 6 depicts the pool-average power spectra of the body angle and ankle torque fluctuation (frequency range up to the noise floor). The pool-average twitch contraction time T – the parameter that would be most likely affected by the choice of cut-off frequency of the applied low-pass filter – did not significantly change for the different filter scenarios (as confirmed by the ANOVA). This can be explained by the fact that the higher frequency components (>10 Hz) – which presumably originate from noise – had a significantly lower power than the slow frequency components (<1 Hz).

The Nyquist stability analysis demonstrated that the identified parameters (T, K, Kp, and Kd) along with the pre-set parameters (B = 5 Nms/rad, τ_F, and τ_M) yielded a stable system for all fourteen subjects when implemented in the previously used closed-loop feedback model of quiet stance [14]. The results of the simulation component indicate that the parameters of the perturbed closed-loop feedback model could be identified reliably when using the simulated time series (Fig. 7). In particular, the coefficients of determination (R^2) for the parameters T and K were both 99.9 %; Kp and Kd were on average slightly over- and underestimated, with R^2 values of 96.3 % and 99.8 %, respectively (Fig. 7). A paired t-test finally revealed no significant differences ($\alpha = 0.1$) between the parameters implemented in the closed-loop model and the parameters identified via the optimization models (Models I and II).

IV. DISCUSSION

One of the two most significant results obtained from the torque matching procedure is that the active and passive torque mechanisms depicted in Fig. 2 can accurately generate the physiological ankle torque fluctuation during quiet stance. The identified torque contributions from the two mechanisms reveal that not only the passive, but also the active ankle torque mechanism contributes significantly to the total ankle torque and, hence, to body stabilization. A second significant result was that the neural-mechanical control scheme shown in Fig. 3 successfully mimics the physiological control strategy during quiet stance and that a PD controller is a legitimate model for the strategy that the CNS applies to regulate the active ankle torque in spite of a long sensory-motor time delay.

For both models, the high level of matching between the experimental and predicted ankle torque could not only be achieved during the optimizations, but also when the identified parameters were used with new sets of data (validations). In fact, no differences in *%Fit* were found between the optimized and validated data. Another common measure for quantifying the fit between two time series, the *Variance Accounted For (%VAF)* [32], [42]-[44], yielded even better results: for both models, *%VAF* had mean values of over 99.9 % and 99.7 % for the optimizations and validations, respectively.

Also other studies have attempted to characterize the balance control scheme during quiet stance [8]-[10], [24], [45]. The present study is unique, however, as it identifies: 1) the active and passive torque contributions; and 2) the parameters of a stable neural-mechanical control scheme that accurately predicts the physiological ankle torque fluctuation while considering the stability-threatening NMS dynamics [14]. Note that the obtained parameters cannot only evoke the physiological ankle torque, but also ensure a stable system for all subjects when used in a closed-

loop feedback model of quiet stance [14].

A.   *Characteristics of Active and Passive Torque Mechanisms*

The identification of the torque mechanisms revealed that the mechanical controller alone cannot yield an optimal fit between the measured and predicted ankle torque. In spite of the permitted optimization ranges for K (up to 150 % of T_{LOAD}) and G (including 0 Nm/V), the identified stiffness gain K of the mechanical controller accounted for only 83 % of the subjects' average load stiffness (*see Table I*). Loram and Lakie [8] and Casadio *et al.* [9] measured the ankle stiffness using small postural perturbations and suggested that K can have a value between 64 % [9] and 91 % [8] of the load stiffness during standing. Morasso and Sanguineti [7] estimated the potential contribution of K as 60 % of the load stiffness based on a simulation study and previously reported values. While our result agrees with these experimental findings on the ankle stiffness, it provides more concrete evidence that most, but not all of the required ankle torque *during standing* is generated by the passive torque mechanism. In fact, between 68 and 91 % of the stabilizing torque is delivered by the passive torque mechanism and, as such, not subject to the phase delay induced by the NMS dynamics and the other feedback time delays. Our findings emphasize, however, that the passive torque cannot stabilize the body alone, and that stability during quiet standing is achieved with the help of a neural control mechanism at the CNS level.

The high *%Fit* in the optimization of the torque mechanisms also proved that the adopted second-order system characterized the NMS dynamics from plantar flexion activation (EMG_{SOL}) to active ankle torque very well. The identified twitch contraction time of 167 ms (*see Table I*) agrees with our previous study in which T was identified using a different methodology (152 ms on average) [14]. Although other T values reported for SOL (86-125 ms) [33], [34], [46] are

smaller than the value of the present study, this can be attributed to the fact that they were obtained during a sitting [33], [46] or prone position [34], i.e., when the ankle joint and muscle conditions are unlike those during standing. In addition, also the motor tasks in these studies were very different compared to standing as they were characterized by the exertion of impulsive voluntary torque at 30 % of maximum voluntary contraction [33] and the application of electrical stimulation [34], [46]. In this context, we believe that smaller T values would have been found for the non-filtered time series if the ankle torque had exhibited more power at higher frequencies. Our results, however, agree with previous studies, indicating that the kinematics and torque data during quiet standing are dominated by very slow frequency components of up to 1 Hz (e.g., [26], [47]).

Also Kearney and his colleagues studied active and passive torque mechanisms of the human ankle joint [44], [48]. In their work, a parallel-cascade system identification method was used to successfully separate and characterize intrinsic and reflex stiffness components that contribute to the overall ankle joint stiffness during position perturbations [44]. While the properties of the intrinsic stiffness component closely resemble those of the passive torque mechanism in the present work (e.g., elastic and viscous components), the identified parameter values differ significantly due to differences in ankle joint position, load, and muscle activation level [14], [48]. In addition, a stiffness component originating from *peripheral* reflex mechanisms should not be present during quiet standing as the sensitivity of the muscle spindle afferents is too low [44] to detect the slow ankle joint motion during body sway [26]. In fact, the contribution of local stretch and other reflexes during quiet standing has been ruled out by Loram *et al.* on the basis of timing [17]. Consequently, also the static nonlinearity in form of a unidirectional rate-sensitive element should not contribute to the ankle joint dynamics during

quiet standing. In a broader sense, the active torque mechanism described in the present study may yet be understood as a form of stiffness mechanism that is continuously [49]-[51] or intermittently [17], [52] regulated by higher centers of the CNS. From this point of view, the studies by Kearney *et al.* [44] and our team are similar in the way that they both identify the contribution of intrinsic and neural mechanisms to the ankle torque generation (for different tasks), and this by analyzing experimental data within a modeling framework.

B.   *Characteristics of Neural Controller within Neural-Mechanical Control Scheme*

The average values for Kp and Kd were 126 Nm/rad and 158 Nms/rad, respectively (*see Table I*). The implication that the average Kp/Kd ratio with a value of 0.8 s^{-1} is relatively small when compared to conventionally implemented PD controllers shows that the Kd gain plays a significant role in the neural controller: it needs to compensate for the stability-threatening sensory-motor time delay, which has been suggested to be much longer than previously assumed due to the delay effect of the NMS dynamics (larger than 280 ms) [14]. Note that the Kp/Kd ratio is even smaller than in our previous study [24] since it investigated only the potential of the neural PD controller without considering the contribution of the mechanical controller. Therefore, the Kp/Kd ratio had to be higher in that study [24] to account for the predominant effect of the mechanical stiffness gain K that is much higher than the mechanical damping gain B.

Finally, we emphasize that the proposed PD control strategy within the neural-mechanical control scheme is a *descriptive* model that can mimic the behavior of the neural controller. As such, it does not necessarily represent the actual neural control system during quiet stance. To realize this concept, predictive [12], adaptive [13], and internal model [20] control mechanisms have been proposed. The actual neural control system, however, that elicits the

active torque component should be investigated in future studies.

Nevertheless, the proposed descriptive control scheme can become very useful when designing prostheses and neuroprostheses for standing (see also [2] and [25]). To accomplish this goal, many other challenges need yet to be addressed. These include the implementation of a sensor for measuring balance and the prevention of foot movement during standing, the reduction of FES induced muscle fatigue, and the selection of the muscles that need to be actuated by means of FES to generate the required torques at different joints (ankle, knee, and hip). The last challenge is additionally complicated by the fact that some of the targeted muscles are actually two joint muscles, making the regulation of particular joints more complex.

C.   *Limitations*

In the present study, the parameters of the neural-mechanical control scheme were identified by minimizing the error between the experimental and predicted ankle torque data. Since these so-called optimizations do not guarantee that the true values are found, the obtained results have to be interpreted with care. It has to be emphasized, however, that the determined values: 1) lie in physiological ranges; 2) ensure a stable closed-loop feedback system; and 3) are in agreement with previous experimental findings [8], [9], [14], [45].

One of the main limitations of the present study is that parameter identifications using closed-loop systems may result in incorrect structures as well as parameter estimates, and that differences in estimates with/without external perturbations may reflect either differences in the system or in estimation. In particular, parameters identified during *quiet* standing may depend on the frequency content of *internal* perturbations [53], which cannot be measured. Consequently, it has been suggested that *external* perturbations are needed to study the closed-loop control of quiet stance [53]. The actual dynamic and control properties of quiet standing may, however, not

be identical to the ones when quiet standing is perturbed via external sensory or mechanical perturbations. Therefore, we believe that it is yet beneficial to study a closed-loop system such as quiet standing without applying external perturbations – while acknowledging that the acquired system parameters may potentially be biased [53]. Most importantly, the results of the simulation component of this study provide strong evidence that the parameters of the feedback system could be identified reliably (Fig. 7) when using the perturbation characteristics (dynamics and entry point) from our previous study [24].

The optimized parameters exhibited a high level of variation among the fourteen subjects. This variation can be explained by the fact that particular subject characteristics that vary from subject to subject have a strong influence on the obtained parameters. They include, for example, the subject anthropometrics (K, Kp, and Kd) and the mechanical properties of the ankle joints and muscles (T and K). Note that the variation of the control gains (K, Kp, and Kd) is in agreement with our previous study, which demonstrated that a considerable gain variation will not threaten the stability of the system [14].

For the identification of the NMS dynamics, we adopted a single muscle model based on the assumption that SOL is the most important contributor to the ankle extension torque. The high *%Fit* in the optimization analysis (Model I) proved that this assumption was appropriate. However, one has to acknowledge that also the gastrocnemius muscle shows some minor activity during standing, which must somehow contribute to the overall torque generation. Nevertheless, the influence of the NMS dynamics on the control mechanism of quiet standing is believed to remain very significant.

V. CONCLUSIONS

Our results provide strong evidence that not only the passive, but also the active ankle torque mechanism contributes significantly to the total ankle torque and, hence, to body stabilization during quiet stance. In addition, we conclude that the proposed neural-mechanical control scheme successfully mimics the physiological control concept during quiet stance. Taking our previous findings into account, we suggest that a PD control strategy is a legitimate model for the strategy that the CNS of healthy individuals applies in order to regulate balance during quiet standing. Supported by our fitting results, we believe that a control scheme that considers the mechanical controller and utilizes neural PD control gains with a relatively small K_p/K_d ratio can, in fact, overcome a large sensory-motor time delay and stabilize the body during quiet stance. The future goal is to implement this control strategy in combination with an FES system to assist individuals with SCI to perform ADL while standing.

ACKNOWLEDGMENT

REFERENCES

[1]   P. H. Veltink and N. Donaldson, "A perspective on the control of FES-supported standing," *IEEE Trans. Rehab. Eng.*, vol. 6(2), pp. 109-112, 1998.

[2]   A. H. Vette, K. Masani, J.-Y. Kim, and M. R. Popovic, "Closed-loop control of FES-assisted arm-free paraplegic standing: A feasibility study," *Neuromodulation*, vol. 12(1), pp. 22-32, 2009.

[3]   J.-Y. Kim, J. K. Mills, A. H. Vette, and M. R. Popovic, "Optimal combination of minimum degrees of freedom to be actuated in the lower limbs to facilitate arm-free paraplegic standing," *ASME J. Biomech. Eng.*, vol. 129(6), pp. 838-847, 2007.

[4]   J. J. Abbas and H. J. Chizeck, "Feedback control of coronal plane hip angle in paraplegic subjects using functional neuromuscular stimulation," *IEEE Trans. Biomed. Eng.*, vol. 38(7), pp. 687-698, 1991.

[5]   R.-P. Jaime, Z. Matjačić, and K. J. Hunt, "Paraplegic standing supported by FES-controlled ankle stiffness," *IEEE Trans. Neural Sys. Rehab. Eng.*, vol. 10(4), pp. 239-248, 2002.

[6]   W. H. Gage, D. A. Winter, J. S. Frank, and A. L. Adkin, "Kinematic and kinetic validity of the inverted pendulum model in quiet standing," *Gait & Posture*, vol. 19, pp. 124-132, 2004.

[7]   P. G. Morasso and V. Sanguineti, "Ankle muscle stiffness alone cannot stabilize balance during quiet standing," *J. Neurophysiol.*, vol. 88, pp. 2157-2162, 2002.

[8]   I. D. Loram and M. Lakie, "Direct measurement of human ankle stiffness during quiet standing: the intrinsic mechanical stiffness is insufficient for stability," *J. Physiol.*, vol. 545, pp. 1041-1053, 2002.

[9]   M. Casadio, P. G. Morasso, and V. Sanguineti, "Direct measurement of ankle stiffness during quiet standing: implications for control modelling and clinical application," *Gait & Posture*, vol. 21, pp. 410-424, 2005.

[10] R. J. Peterka, "Sensorimotor integration in human postural control," *J. Neurophysiol.*, vol. 88, pp. 1097-1118, 2002.

[11] R. J. Peterka, "Postural control model interpretation of stabilogram diffusion analysis,"

Biol. Cybern., vol. 82, pp. 335-343, 2000.

[12] H. van der Kooij, R. Jacobs, B. Koopman, and H. Grootenboer, "A multisensory integration model of human stance control," *Biol. Cybern.*, vol. 80, pp. 299-308, 1999.

[13] H. van der Kooij, R. Jacobs, B. Koopman, and F. van der Helm, "An adaptive model of sensory integration in a dynamic environment applied to human stance control," *Biol. Cybern.*, vol. 84, pp. 103-115, 2001.

[14] K. Masani, A. H. Vette, N. Kawashima, and M. R. Popovic, "Neuro-musculo-skeletal torque generation process has a large destabilizing effect on the control mechanism of quiet standing," *J. Neurophysiol.*, vol. 100, pp. 1465-1475, 2008.

[15] I. D. Loram, C. N. Maganaris, and M. Lakie, "Paradoxical muscle movement in human standing," *J. Physiol.*, vol. 556, pp. 683-689, 2004.

[16] I. D. Loram, C. N. Maganaris, and M. Lakie, "Active, non-springlike muscle movements in human postural sway: How might paradoxical changes in muscle length be produced?," *J. Physiol.*, vol. 564, pp. 281-293, 2005.

[17] I. D. Loram, C. N. Maganaris, and M. Lakie, "Human postural sway results from frequent, ballistic bias impulses by soleus and gastrocnemius," *J. Physiol.*, vol. 564(1), pp. 295-311, 2005.

[18] R. Fitzpatrick, D. Burke, and S. C. Gandevia, "Loop gain of reflexes controlling human standing measured with the use of postural and vestibular disturbances," *J. Neurophysiol.*, vol. 76, pp. 3994-4008, 1996.

[19] P. Gatev, S. Thomas, T. Kepple, and M. Halett, "Feedforward ankle strategy of balance during quiet stance in adults," *J. Physiol.*, vol. 514, pp. 915-928, 1999.

[20] P. G. Morasso, L. Baratto, R. Capra, and G. Spada, "Internal models in the control of posture," *Neural Networks*, vol. 12, pp. 1173-1180, 1999.

[21] R. J. Peterka, "Posture control: Simplifying the complexities of maintaining balance. Insights provided by simple closed-loop models of human postural control," *IEEE Eng. Med. Biol. Mag.*, vol. 22, pp. 63-68, 2003.

[22] R. Johansson, M. Magnusson, and M. Akesson, "Identification of human postural

dynamics," *IEEE Trans. Biomed. Eng.*, vol. 35, pp. 858-869, 1988.

[23] K. Masani, M. R. Popovic, K. Nakazawa, M. Kouzaki, and D. Nozaki, "Importance of body sway velocity information in controlling ankle extensor activities during quiet stance," *J. Neurophysiol.*, vol. 90, pp. 3774-3782, 2003.

[24] K. Masani, A. H. Vette, and M. R. Popovic, "Controlling balance during quiet standing: proportional and derivative controller generates preceding motor command to body sway position observed in experiments," *Gait & Posture,* vol. 23, pp. 164-172, 2006.

[25] A. H. Vette, K. Masani, and M. R. Popovic, "Implementation of a physiologically identified PD feedback controller for regulating the active ankle torque during quiet stance," *IEEE Trans. Neural Sys. Rehab. Eng.*, vol. 15, pp. 235-243, 2007.

[26] D. A. Winter, *Biomechanics and motor control of human movement*. New York: Wiley & Sons, 2005, ch. 2-6.

[27] V. P. Panzer, S. Bandinelli, and M. Hallett, "Biomechanical assessment of quiet standing and changes associated with aging," *Arch. Phys. Med. Rehabil.*, vol. 76, pp. 151-157, 1995.

[28] G. T. Yamaguchi, A. G. U. Sawa, D. W. Moran, M. J. Fessler, and J. M. Winters, "A survey of human musculotendon actuator parameters. In: *Multiple Muscle Systems*, edited by J. M. Winters and S.-Y. Woo. New York: Springer-Verlag, 1990, pp. 716-773.

[29] A. Mannard and R. B. Stein, "Determination of the frequency response of isometric soleus muscle in the cat using random nerve stimulation," *J. Physiol.*, vol. 229, pp. 275-296, 1973.

[30] R. B. Stein, A. S. French, A. Mannard, and R. Yemm, "New methods for analysing motor function in man and animals," *Brain Res.*, vol. 40, pp. 187-192, 1972.

[31] A. J. Fuglevand, D. A. Winter, and A. E. Patla, "Models of recruitment and rate coding organization in motor-unit pools," *J. Neurophysiol.*, vol. 70, pp. 2470-2488, 1993.

[32] T. Ito, E. Z. Murano, and H. Gomi, "Fast force-generation dynamics of human articulatory muscles," *J. Appl. Physiol.*, vol. 96, pp. 2318-2324, 2004.

[33] H. Tani and H. Nagasaki, "Contractile properties of human ankle muscles determined by a systems analysis method for the EMG-force relationship," *J. Electromyogr. Kinesiol.*, vol.

6(3), pp. 205-213, 1996.

[34] P. Bawa and R. B. Stein, "Frequency response of human soleus muscle," *J. Neurophysiol.*, vol. 39(4), pp. 788-793, 1976.

[35] Y. Kawakami, Y. Ichinose, and T. Fukunaga, "Architectural and functional features of human triceps surae muscles during contraction," *J. Appl. Physiol.*, vol. 85, pp. 398-404, 1998.

[36] J. Bobet and R. B. Stein, "A simple model of force generation by skeletal muscle during dynamic isometric contractions," *IEEE Trans. Biomed. Eng.*, vol. 45, pp. 1010-1016, 1998.

[37] F. E. Zajac, "Muscle and tendon: properties, models, scaling, and application to biomechanics and motor control," *Crit. Rev. Biomed. Eng.*, vol. 17, pp. 359-411, 1989.

[38] C. Applegate, S. C. Gandevia, and D. Burke, "Changes in muscle and cutaneous cerebral potentials during standing," *Exp. Brain Res.*, vol. 71, pp. 183-188, 1988.

[39] B. A. Lavoie, F. W. J. Cody, and C. Capaday, "Cortical control of human soleus muscle during volitional and postural activities studied using focal magnetic stimulation," *Exp. Brain Res.*, vol. 103, pp. 97-107, 1995.

[40] N. Accornero, M. Capozza, S. Rinalduzzi, and G. W. Manfredi, "Clinical multisegmental posturography: age-related changes in stance control," *Electroencephalogr. Clin. Neurophysiol.*, vol. 105, pp. 213–219, 1997.

[41] C. D. Perttunen, D. R. Jones, and B. E. Stuckman, "Lipschitzian optimization without the lipschitz constant," *J. Optimiz. Theory and Appl.*, vol. 79(1), pp. 157-181, 1993.

[42] I. D. Loram and M. Lakie, "Human balancing of an inverted pendulum: position control by small, ballistic-like, throw and catch movements," *J. Physiol.*, vol. 540(3), pp. 1111-1124, 2002.

[43] K. M. Moorhouse and K. P. Granata, "Role of reflex dynamics in spinal stability: Intrinsic muscle stiffness alone is insufficient for stability," *J. Biomech.*, vol. 40, pp. 1058-1065, 2007.

[44] R. E. Kearney, R. B. Stein, and L. Parameswaran, "Identification of intrinsic and reflex contributions to human ankle stiffness dynamics," *IEEE Trans. Biomed. Eng.*, vol. 44(6),

pp. 493-504, 1997.

[45] P. G. Morasso and M. Schieppati, "Can muscle stiffness alone stabilize upright standing?," *J. Neurophysiol.*, vol. 82, pp. 1622-1626, 1999.

[46] F. Bellemare, J. J. Woods, R. Johansson, and B. Bigland-Ritchie, "Motor unit discharge rates in maximal voluntary contractions in three human muscles," *J. Neurophysiol.*, vol. 50, pp. 1380-1392, 1983.

[47] R. C. Fitzpatrick, R. B. Gorman, D. Burke, and S. C. Gandevia, "Postural proprioceptive reflexes in standing human subjects: bandwidth of response and transmission characteristics," *J. Physiol.*, vol. 458, pp. 69-83, 1992.

[48] M. M. Mirbagheri, H. Barbeau, and R. E. Kearney, "Intrinsic and reflex contributions to human ankle stiffness: variation with activation level and position," *Exp. Brain Res.*, vol. 135, pp. 423-436, 2000.

[49] T. Kiemel, A. J. Elahi, and J. J. Jeka, "Identification of the plant for upright stance in humans: multiple movement patterns from a single neural strategy," *J. Neurophysiol.*, vol. 100(6), pp. 3394-3406, 2008.

[50] H. van der Kooij and E. de Vlugt, "Postural responses evoked by platform perturbations are dominated by continuous feedback," *J. Neurophysiol.*, vol. 98(2), pp. 730-743, 2007.

[51] T. Kiemel, K. S. Oie, and J. J. Jeka, "Slow dynamics of postural sway are in the feedback loop," *J. Neurophysiol.*, vol. 95(3), pp. 1410-1418, 2006.

[52] A. Bottaro, Y. Yasutake, T. Nomura, M. Casadio, and P. Morasso, "Bounded stability of the quiet standing posture: an intermittent control model," *Hum. Mov. Sci.*, vol. 27(3), pp. 473-495, 2008.

[53] H. van der Kooij, E. van Asseldonk, and F. C. T. van der Helm, "Comparison of different methods to identify and quantify balance control," *J. Neurosci. Methods*, vol. 145, pp. 175-203, 2005.

TABLE I. OPTIMIZATION RESULTS FOR MODEL I (ACTIVE AND PASSIVE TORQUE MECHANISMS) AND MODEL II (NEURAL-MECHANICAL CONTROL SCHEME)

| Model	Parameter/Fit		Inter-Subject Values		Intra-Subject Variation (SD)		$\dfrac{SD_{Intra}}{SD_{Inter}}$
			Mean	*SD*	*Mean*	*SD*	
I	T	[ms]	167	29	6	2	21%
	G	[Nm/V]	58	37	2	3	5%
	K	[Nm/rad]	521	95	4	6	4%
		[%T$_{LOAD}$]	83	7	< 1	< 1	4%
	%Fit Opt	[%]	98.4	0.5	–	–	–
	%Fit Val	[%]	96.7	2.9	–	–	–
II	Kp	[Nm/rad]	126	47	4	6	9%
	Kd	[Nms/rad]	158	71	9	5	13%
	%Fit Opt	[%]	98.3	0.5	–	–	–
	%Fit Val	[%]	96.6	3.6	–	–	–
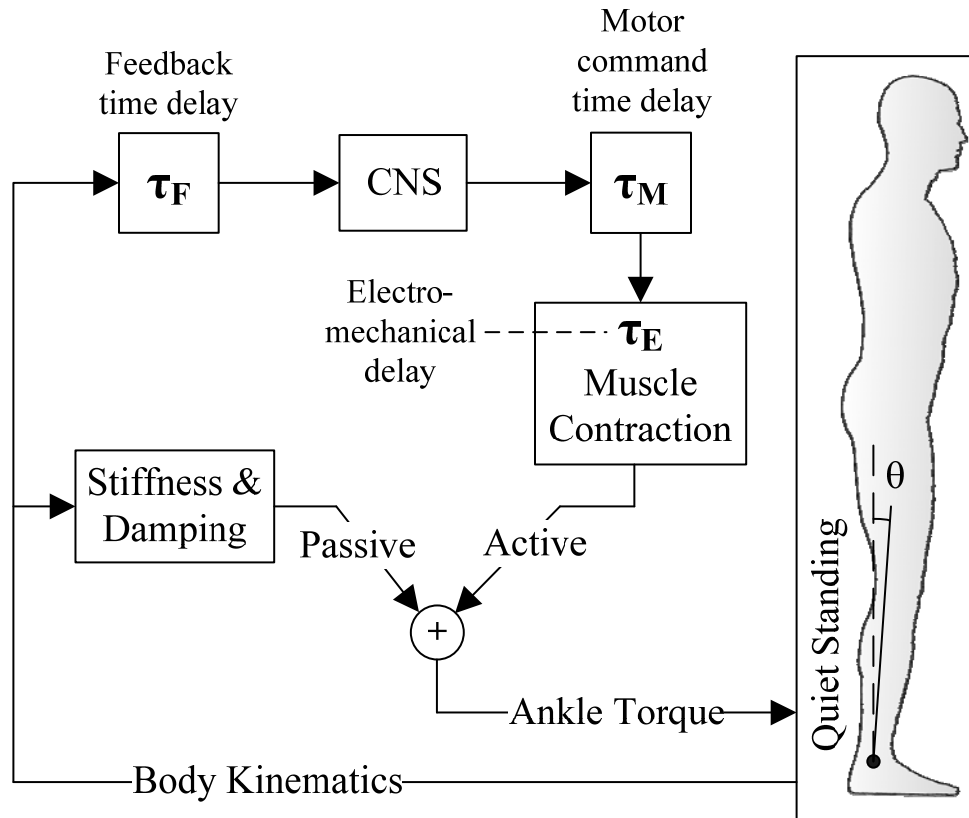
Fig. 1. Neural-mechanical control concept of quiet standing. The passive torque depends on the rotational ankle joint, muscle, and ligament properties (stiffness and damping), whereas the active torque is regulated by the CNS via the body kinematics and generated by the contractions of the plantar flexors. Since the sensory-motor time delay within the neural feedback loop (τ_F + τ_M + τ_E) threatens the stability of the system, it has to be compensated for by the neural controller.
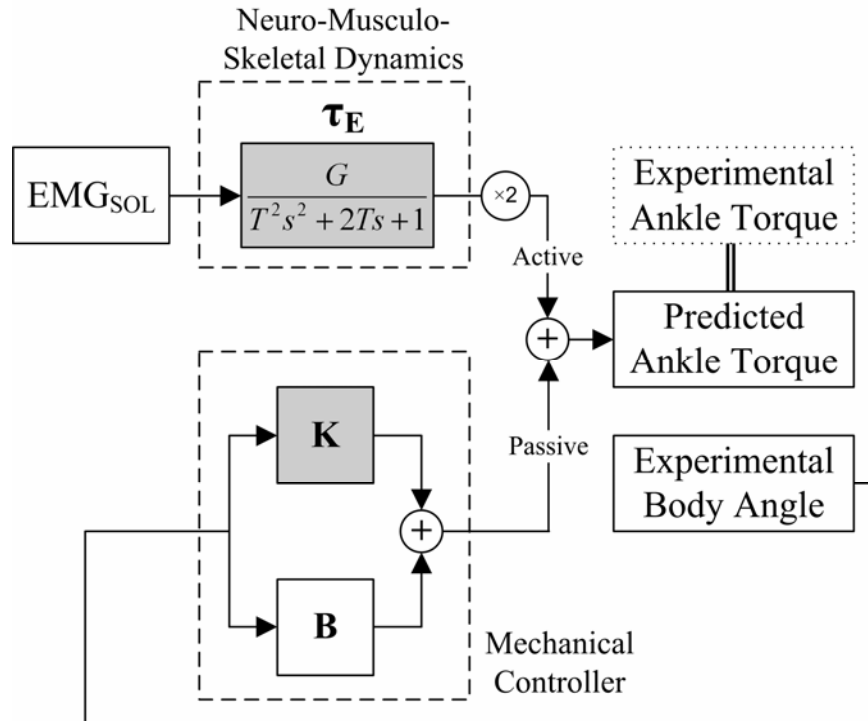
Fig. 2. Model of the NMS dynamics and the mechanical controller. A critically damped, second-order low-pass system was used to model the NMS dynamics between muscle activation and active ankle torque (upper dashed box). The mechanical controller with gains for the rotational stiffness (K) and damping (B) generated the passive ankle torque based on the body angle fluctuation during quiet standing (lower dashed box).
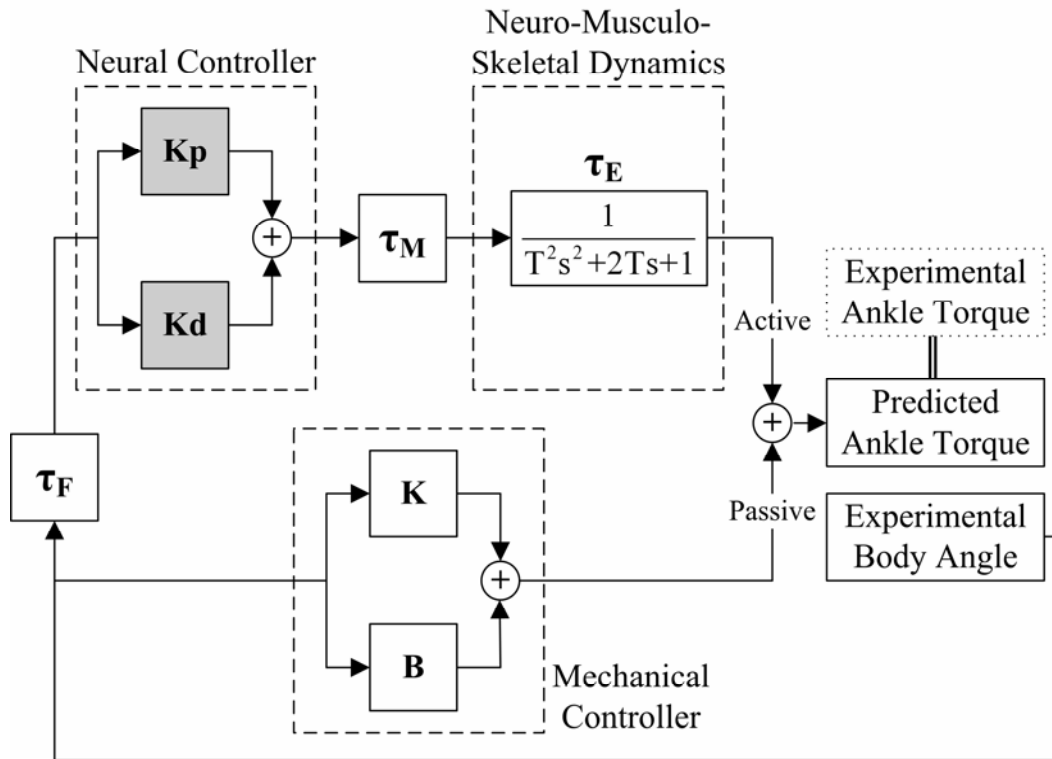
Fig. 3. Feedback model of the neural-mechanical control scheme of quiet standing. The neural PD controller (upper left dashed box) generated the motor command for the plantar flexors (upper right dashed box) based on sensory information about the body kinematics. The resulting active ankle torque in addition to the passive ankle torque from the mechanical controller (lower dashed box) yielded the total ankle torque fluctuation.
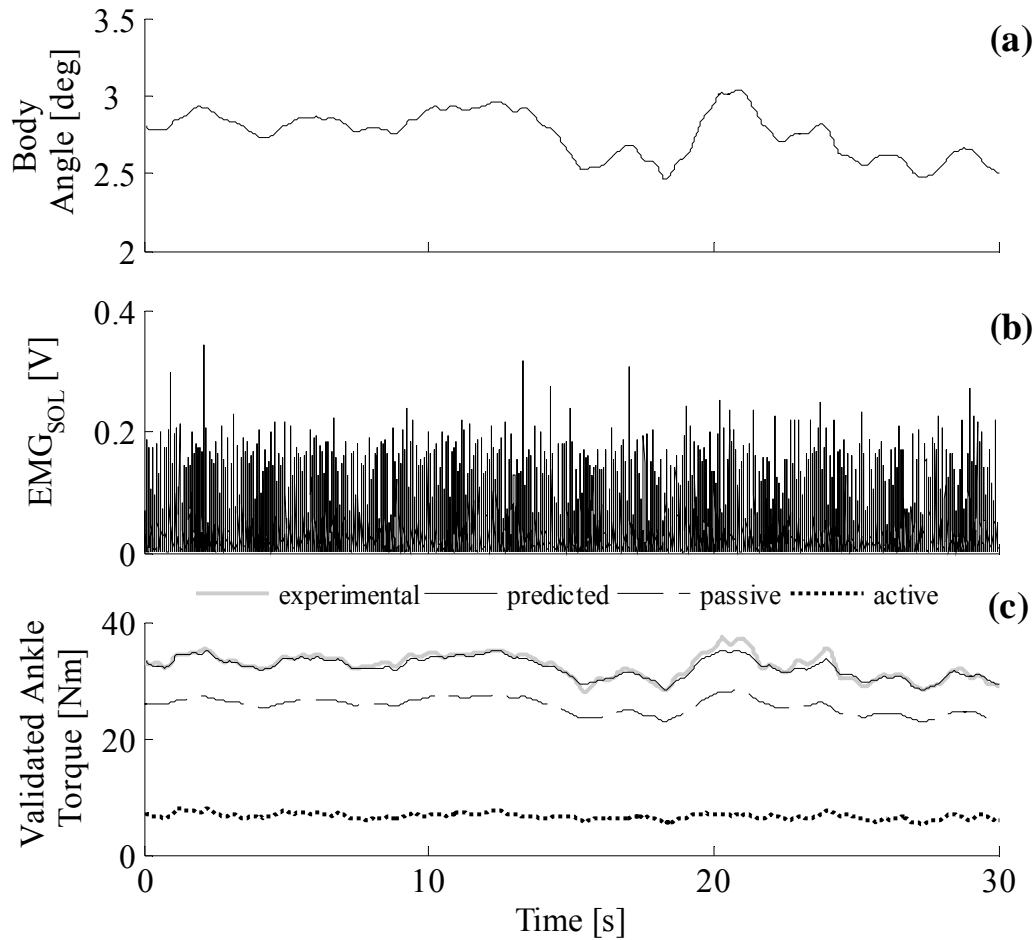
Fig. 4. Experimental time series and ankle torque predicted via the active and passive torque mechanisms depicted in Fig. 2 (validation). Shown are the fluctuation of the body angle (a), the right EMG_{SOL} (b), and the experimental ankle torque (bold gray line) and predicted ankle torque (thin black line) (c). The dashed and dotted lines in Fig. 4c represent the predicted passive and active torque components, respectively.
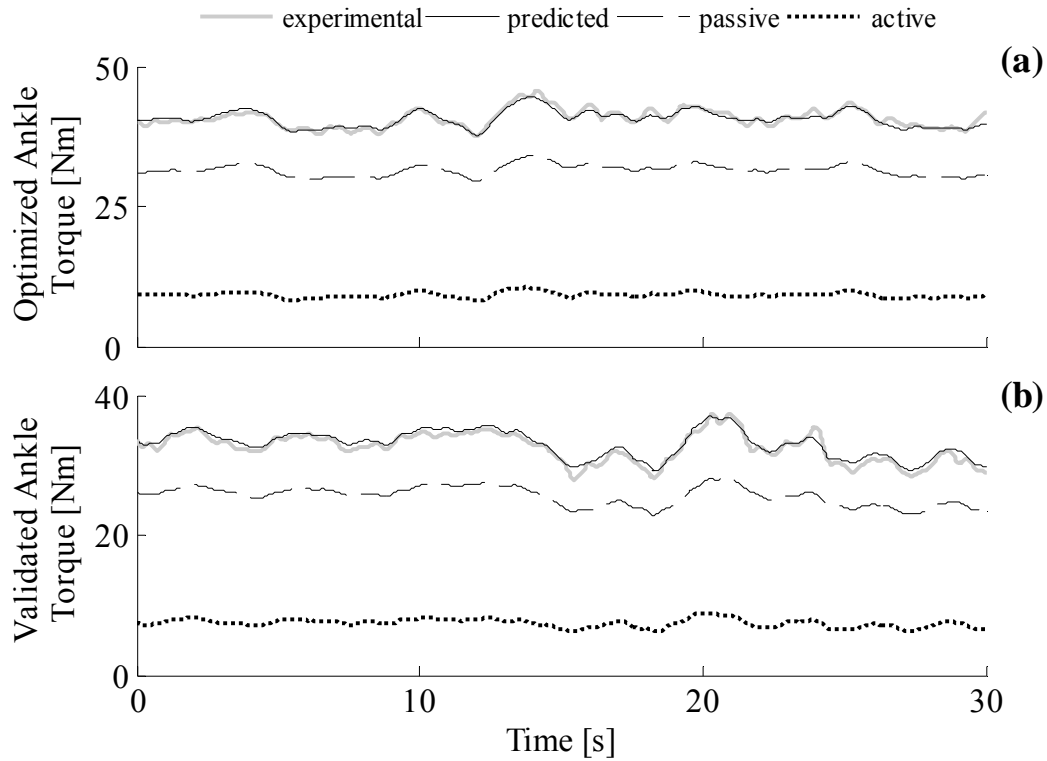
Fig. 5. Ankle torque fluctuation from experiments (bold gray lines) and predicted via the model of the neural-mechanical control scheme (thin black lines). The dashed and dotted lines represent the predicted passive and active torque components, respectively. Fig. 5a shows the ankle torque fluctuation from the optimization trial and Fig. 5b from the validation trial.
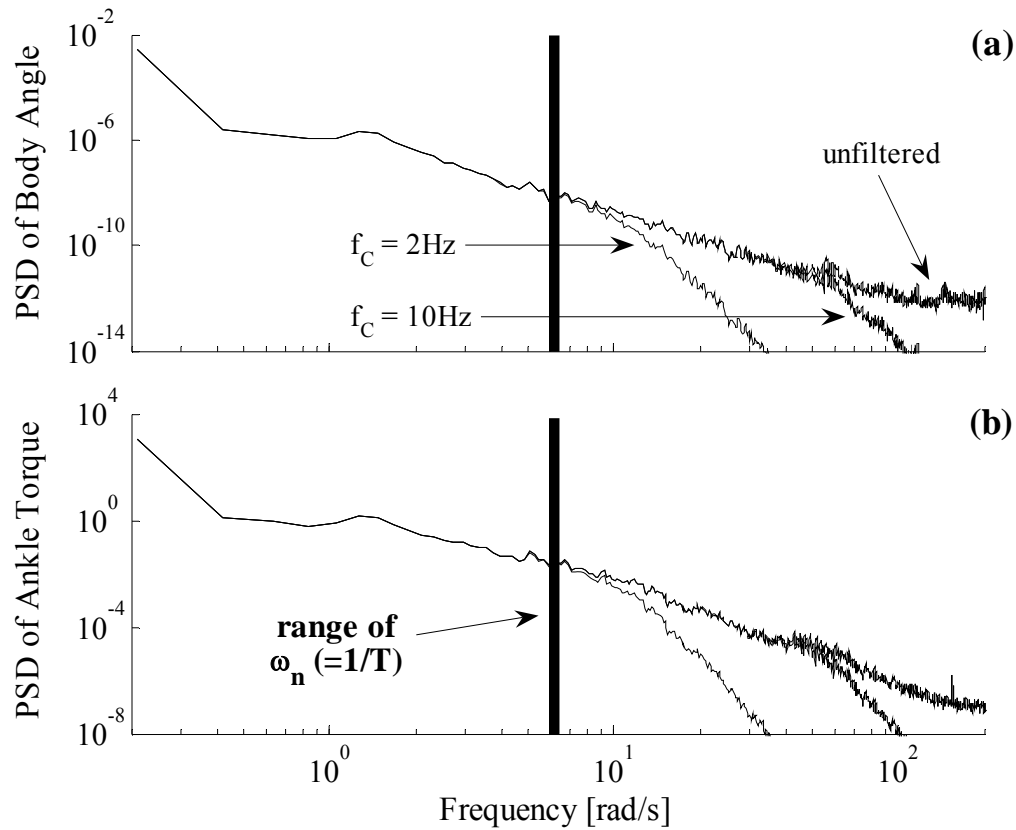
Fig. 6. Pool-average power spectra of body angle (a) and ankle torque fluctuation (b). The pool-average twitch contraction time T (or the system's natural frequency ω_n) did not significantly change with different cut-off frequencies (f_c) of the low-pass filter (body angle and ankle torque).
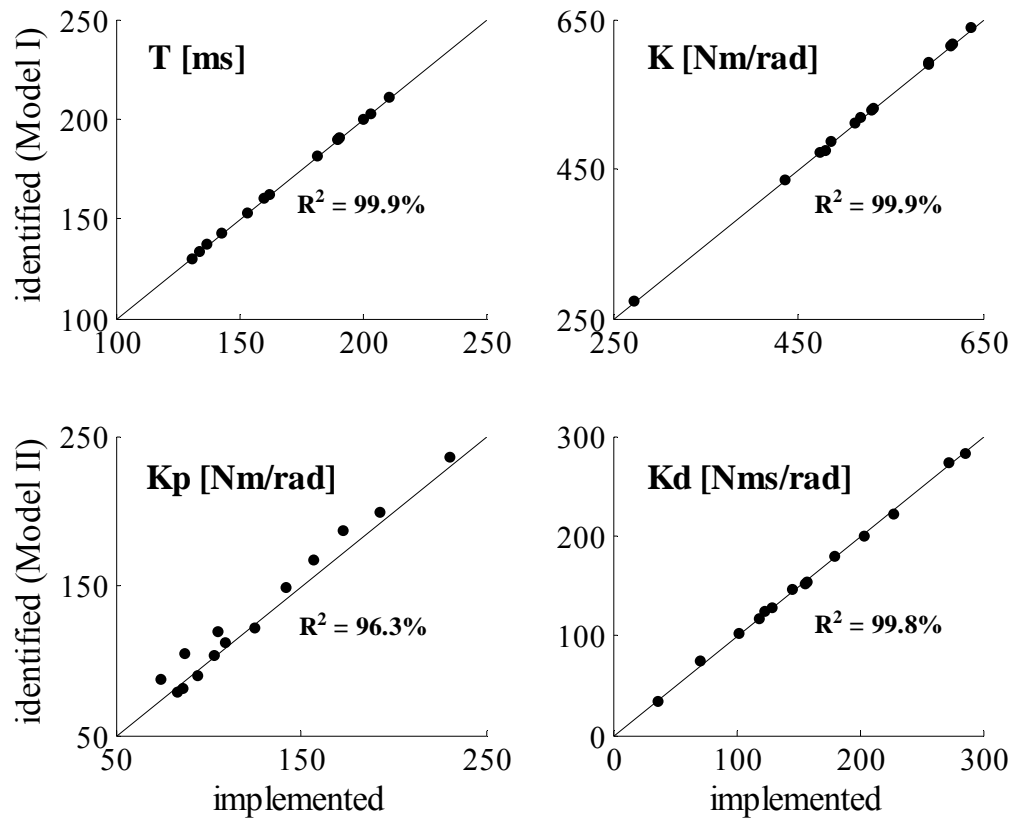
Fig. 7. Results of the model structure and parameter verification. A good fit was found between the parameters implemented in the closed-loop feedback model and those optimized via the optimization models (Models I and II). The subjects' parameters T and K had both an R^2 value of 99.9 %; Kp and Kd were on average slightly over- and underestimated, with R^2 values of 96.3 % and 99.8 %, respectively.